ENHANCING STEM CELL DELIVERY TO THE TRABECULAR MESHWORK USING MAGNETIC NANOPARTICLES

A Thesis
Presented to
The Academic Faculty

by

Kelsey Tweed

In Partial Fulfillment
of the Requirements for the Degree
Bachelor of Science with the Research Option in the
School of Biomedical Engineering

Georgia Institute of Technology
May 2018

ENHANCING STEM CELL DELIVERY TO THE TRABECULAR MESHWORK USING MAGNETIC NANOPARTICLES

Approved by:

Ross Ethier

Lisa Schildmeyer

Eric Snider

Date Approved: 4/19/2018

ACKNOWLEDGEMENTS

I wish to thank everyone in the Ethier Lab at Georgia Tech, especially Dr. Eric Snider, my graduate student mentor, and principal investigator Dr. Ross Ethier, for providing me the opportunity to conduct this research as well as providing their support, assistance, and mentorship throughout my time working in the lab. Additionally, I would like to thank Lisa Schildmeyer for supporting my research and serving as a committee member. Finally, I would also like to especially thank my mother and father, without whose guidance and support I would not be here.

TABLE OF CONTENTS

LIST OF FIGURES

LIST OF SYMBOLS AND ABBREVIATIONS

OAG	open-angle glaucoma
AH	aqueous humor
TM	trabecular meshwork
SC	Schlemm's canal
IOP	intraocular pressure
ADSC	adipose derived mesenchymal stem cells
iPSC	induced pluripotent stem cells
PBNC	Prussian blue nanocubes
FBS	fetal bovine serum
CFSE	carboxyfluorescein succinimidyl ester

SUMMARY

The trabecular meshwork (TM) is a structure in the eye responsible for the drainage of aqueous humor. Due to the reduced cellularity found in the TM during glaucoma, TM function is reduced, resulting in elevated intraocular pressure. Stem cell therapies could provide a novel treatment option if cell delivery can be targeted to the TM. The purpose of this study is to determine if delivery of stem cells, labeled with Prussian blue magnetic nanocubes, delivered to the TM can be enhanced with magnetic field application. For delivery experiments, anterior segments of porcine eyes, were maintained in organ culture and perfused at physiological flow rates. Stem cells labeled with magnetic nanoparticles were injected intracamerally and steered to the TM region with a magnetic field. Confocal fluorescent imaging showed an increase in the delivery of stem cells to the TM when compared to control with no magnet. This novel technique for delivering stem cells may allow for future research into cell therapies for glaucoma which directly target the TM. Such a treatment could benefit the millions of individuals who suffer from glaucoma.

CHAPTER 1

INTRODUCTION

Glaucoma is a group of eye-related disorders that lead to optic nerve damage and eventual vision loss (1). Open-angle glaucoma (OAG), the most common form of glaucoma, is caused by an increase in resistance to the drainage of aqueous humor (AH) through the trabecular meshwork (TM) and Schlemm's canal (SC)(1). This increased resistance results in elevated intraocular pressure (IOP), damaging the optic nerve, and leading to vision loss. Although a majority of AH drains through the TM/SC, known as the "conventional route", current glaucoma treatments do not directly target this route(2). Instead, drugs either decrease the production of AH or increase flow through the unconventional pathway, which normally only accounts for approximately 10% of AH drainage(1). Thus, methods that target the primary outflow path of AH would be beneficial for the treatment of glaucoma.

TM cells are crucial for the regulation of IOP through modulation of AH drainage resistance, possibly due to constriction or relaxation of the tissue(2). The cellularity of the TM decreases throughout a person's life, up to 60% by age 80(3). The remaining TM cellularity can be further reduced by 30% in cases of glaucoma(4). This loss in cellularity likely prevents the TM from properly functioning, resulting in increased resistance, increased IOP, increasingly worse optic nerve damage, and eventual vision loss. Therapies that aim to reintroduce functional TM cells to the TM have the potential to restore the tissue's ability to properly modulate IOP. To restore TM cellularity, a variety of stem cell sources, such as adipose derived mesenchymal stem cells (ADSCs), and

induced pluripotent stem cells (iPSCs), have been used and shown to have the potential to differentiate into functional TM cells(5, 6). Injections of stem cells into the anterior chamber in various animal models of glaucoma have been shown to reduce IOP(5, 7, 8). However, delivery of stem cells to the TM has been inefficient and, of the delivered cells to the TM, the cells were not consistently retained in the TM for prolonged periods of time, necessitating an enhanced cell delivery method.

One challenge in cell delivery to the TM is that drainage of AH is naturally segmental. At any given time, only approximately one third of the TM region is experiencing flow. As a result, a large majority of injected cells or particles concentrated in that third of the TM(2). It is thought that the actively filtering regions of the TM fluctuate, so cell delivery to all portions of the damaged TM circumference is crucial for glaucoma therapies. However, this is not possible with passive cell delivery. A method is needed to ensure that the cells will be delivered to the entire circumference of the TM instead of congregating only in active filtering regions. In addition, it is important to prevent non-specific delivery to other anterior tissues during stem cell delivery. Stem cell attachment to non-target tissue such as the lens and cornea, has the potential to damage these tissues and impact vision. A method to enhance cell delivery to all regions of the TM while preventing off-target delivery is needed to further study the regenerative potential of stem cells in glaucoma.

To enhance stem cell delivery, we used magnetic nanoparticles. These nanoparticles have been utilized for many different regenerative medicine applications, such as enhancing tissue penetration of drugs or cells to a target tissue by utilizing magnetic fields(9). This study seeks to utilize Prussian blue Nanocubes (PBNCs), a type

of magnetic nanoparticle comprised of superparamagnetic iron oxide nanoparticles and Prussian blue dye which allows for visual detection of particles(10). Stem cells will be labeled with an optimized concentration of PBNCs, as determined by cell viability and function assessment. Labeled stem cells will then be injected into anterior segments of porcine eyes cultured in perfusion dishes to assess if cell delivery to the TM is enhanced with a magnetic field. Specifically, to determine if the injected cells are pulled evenly to the entire circumference of the TM. A method resulting in an even distribution of stem cells delivered to the TM will aid in the creation of a glaucoma treatment that specifically targets the conventional route of AH drainage.

CHAPTER 2

LITERATURE REVIEW

Glaucoma affects over 70 million people worldwide and is the second leading cause of blindness(2). Many glaucoma treatments aim to decrease the production of AH or increase uveoscleral outflow in order to decrease the elevated IOP which is causing damage to the eye(1). Currently, there are no treatments that directly target the TM, the main structure which controls IOP. Stem cells can potentially be used to repopulate and return function to the partially decellularized TM in glaucomatous eyes(3, 5). However, delivering stem cells to the TM with minimal non-specific binding and for long durations needs to be optimized.

Pluripotent vs. Multipotent Stem Cells

Stem cells are an immature cell type which self-renew and have the capacity to differentiate into other cell types(11). Stem cell self-renewal allows them to indefinitely proliferate to more cells of the same type. The key function of stem cells is maturation, or differentiation, to other cell types found throughout the body(12). Totipotent stem cells have the potential to differentiate into any type of adult cell as well as embryological tissue(13). Pluripotent stem cells have the ability to differentiate into any type of adult cells and are harvested from embryos, known as embryonic stem cells, or reprogrammed from adult somatic cells, known as iPSCs (14-16). Some stem cells are more limited in the types of cells that they can differentiate into. These are called multipotent stem cells. Multipotent stem cells are found throughout the body, but are generally isolated from either bone marrow or adipose tissue(11). There are two main types of multipotent stem

cells: mesenchymal and hematopoietic. Mesenchymal stem cells can differentiate into a variety of tissue cell types while hematopoietic stem cells differentiate into blood cells(11, 17). Although multipotent stem cells are more restricted in the types of cells they can differentiate into, they are a great resource for regenerative therapy studies. Multipotent stem cells can be autologous, meaning that the cells can be harvested from the individual who will be receiving the treatment which reduce the chances of rejection(11). ADSCs are especially useful due to the ease of harvesting and abundance of cells obtained at each harvest. Unlike pluripotent stem cells, ADSCs are also non-tumorigenic, meaning they do not have the risk of forming tumors when they are injected into the body; this makes them more attractive for translational clinical studies(11, 14).

Recent Advances in Stem Cell Delivery to the TM

One of the most common issues with current stem cell delivery is a lack of specificity in tissue engraftment(18). For delivery to the TM, off-target cell integration could be detrimental to other structures within the anterior chamber of the eye, such as the lens. According to a study done in mice utilizing iPSCs, off-target integration was observed in the endothelial layer of Schlemm's canal and on the corneal epithelium and stroma, especially in the area directly surrounding the injection site (6). The iPSCs used in this study were first differentiated into iPSC-TM cells, cells resembling functional TM cells, before injection (6). To avoid tumor formation due to pluripotent cells, iPSC-TM cells must be purified from non-differentiated cells prior to injection. If this purification process is not 100 percent successful, tumors may form due to the presence of cells that still retain their pluripotent nature. As a simpler alternative, multiple studies have used adipose tissue as a source of multipotent stem cells capable of differentiating into TM

cells (11, 12). A method that increases delivery efficiency and reduces the non-specific binding of the injected cells is needed to prevent possible damage to anterior chamber structures.

Roubeix et al. found that the distribution of mesenchymal stem cells (ADSCs) is not equal throughout the entirety of the TM (7). Despite this uneven cell delivery, they still observed IOP reduction after ADSC delivery(7). However, delivery to the entirety of the TM may be essential for therapies. In addition, in this study, IOP was only measured every 3-4 days(7). This low sampling rate allows for important information to be missed between measurements. A method that records IOP more frequently would provide more complete data.

According to a study by Manuguerra-Gagne et al.(8), ADSCs injected into the anterior chamber of murine eyes were no longer detectable after 96 hours. This study created a glaucoma model by using a laser to damage portions of the TM to represent the loss of cellularity which occurs in glaucoma(8). The authors found that the injected ADSCs were able to successfully migrate to the area of damaged tissue but did not remain in the anterior chamber for a prolonged period of time(8). Thus, it may follow that a method to increase survival of cells in the TM as well as a method to specify their target region without further damage to the TM is needed.

Potential of Magnetic Nanoparticles

Magnetic nanoparticles are beginning to emerge as a useful tool for regenerative medicine (9). They can be utilized to improve target specificity and enhance penetration of cells into tissues(9). Many types of magnetic nanoparticles have been shown to be nontoxic to cells and suitable for intraocular use(19, 20). Therefore, it is possible that

nanoparticle-labeled stem cells can be used to specifically target the TM and increase penetration into the TM. Ideally, this will enhance stem cell retention in the tissue. In addition, it is possible to detect magnetic nanoparticles using ultrasound and photoacoustic imaging(21). Ultrasound can be used to non-invasively image by aiming high frequency sound waves at objects and interpreting the waves that return to the transducer. Photoacoustic imaging pairs with standard ultrasound by using a laser to energize photoabsorbers, such as many different dyes and pigment, which causes them to expand and produce sound waves detectable by ultrasound. This would be useful for obtaining images of the injection process and for tracking cell delivery in real-time.

This study seeks to utilize Prussian blue nanocubes(PBNCs) (10), a type of magnetic nanoparticle, along with ADSCs to enhance cell engraftment to the TM. An optimal concentration of PBNCs will be determined based on cell viability and proliferation. After this concentration is determined, ADSCs will be labeled with the PBNCs and injected into the anterior segment of porcine eyes set up in custom-built organ culture dishes where they will be perfused at physiological rates. We will then use a ring magnet to guide the injected cells to the TM. We hypothesize that this method will allow for ADSC delivery to the entire TM circumference as well as increase the penetration of the cells into the target tissue. The organ-cultured eyes will be connected to pressure transducers and a computer which records data each minute throughout the entirety of the experiment. This method of stem cell delivery overcome delivery heterogeneity and lessens off-target delivery since most of the cells pull to the correct location due to magnetic field.

CHAPTER 3

METHODS

Cell Culture

Fully characterized human ADSCs from Lonza were grown in α-minimum essential medium supplemented with 20% fetal bovine serum (FBS), penicillin, streptomycin, and L-glutamine. In all experiments, ADSCs are used at passage numbers five or six.

PBNC and Fluorescent Stem Cell Labeling

ADSCs were labeled with 200nm PBNCs by incubating with different optical densities (ODs) of PBNCs ranging from 0 to 2 OD overnight in a 37^{o} C incubator. Before delivery, cells were fluorescently labeled with CFSE (carboxyfluorescein succinimidyl ester). To do this, cells were detached with 0.05% Trypsin/EDTA and resuspended in 5uM CFSE (2mL for ~ 1million cells) for 15 minutes at 37^{o} C. High serum media (20% FBS, 6mL for ~1million cells) was then added to quench unreacted CFSE.

Porcine Eye Dissection

Fresh porcine eyes, sourced from a slaughterhouse, were used within 6-8 hours of enucleation. First, orbital connective tissue was removed, and eyes were soaked in Betadine solution for 5 minutes. Following Betadine immersion, eyes were transferred to a sterile laminar flow hood for the remainder of the process. Eyes were hemisected with a razor blade to isolate the anterior segment. The vitreous humor and lens were removed, the iris was dissected back until the TM was revealed, and the ciliary processes were

carefully removed while preserving the TM. Any additional vascularized, pigmented tissue was then removed.

Porcine Eye Perfusion

Dissected eyes were placed in a custom-designed organ culture dish (Figure 1 A) and secured in place with a ring clamp (Figure 1 B). The dishes containing the eyes were placed in a 37º C incubator and perfused at 2.5 uL/min with serum-free media containing 1x penicillin, streptomycin, and amphotericin while pressure was recorded through transducer readings in LabView (Figure 1 C). Eyes were allowed to stabilize for at least 48 hours before conducting any experiments. Any eyes whose outflow facility was unable to stabilize between 0.45 and 0.125 uL/min/mmHg (~6mmHg to 20mmHg IOP) were not considered for ADSC delivery experiments.

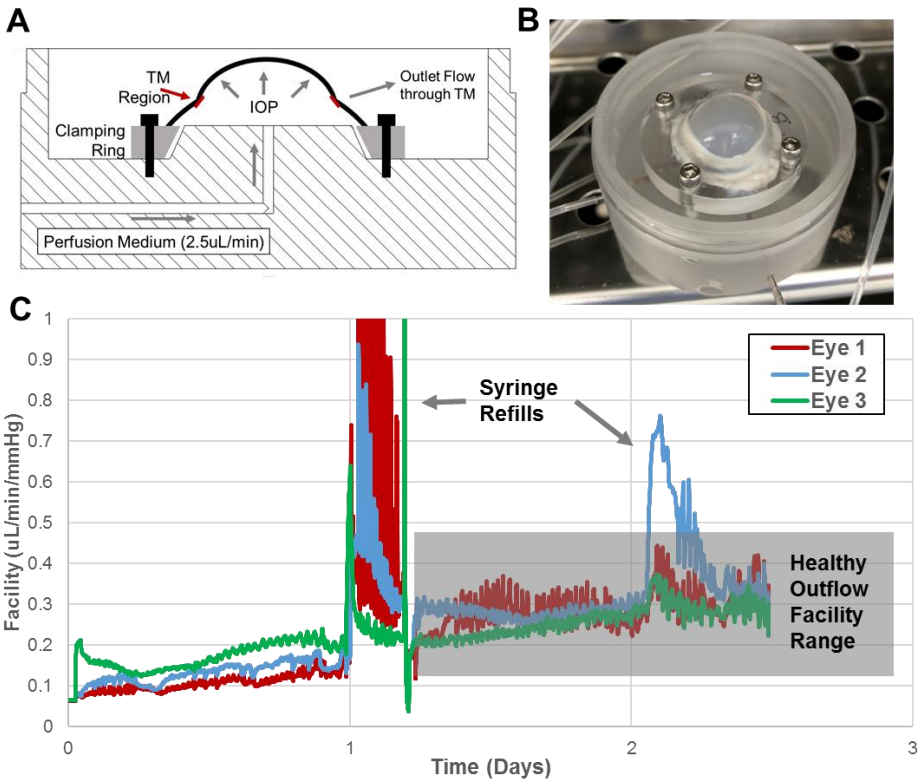

Figure 1. Organ Culture Set Up. (A) Cross section of a custom-built organ culture dish. (B) Anterior segment of a porcine eye clamped into an organ culture dish. (C) Example outflow facility data retrieved from pressure transducer readings.

ADSC injection into Porcine Eyes

250,000 ADSCs (1 million cells/mL) were injected through the center of the cornea while eyes were hydrostatically clamped at 8 to 12 mmHg. A neodymium bar magnet (1" L x 0.25" W x 0.25" H) was used to apply a magnetic field to one quadrant of the TM for either 15 minutes, 30 minutes, 60 minutes, or overnight.

For other experiments, ring magnets were used for delivering stem cells to the entire TM circumference. Two different rings magnets were used. First, a model which houses 10 cylindrical neodymium magnets arranged in a ring and can be set up in the organ culture dishes was constructed in SOLIDWORKS and 3D printed. Second, a

commercially available axially polarized ring magnet was used. After delivery, eyes were then formalin fixed.

Image Processing

After fixation, the sclera was trimmed close to the TM region and placed in a glass bottom 50mm dish for en face imaging of the anterior segment. Micrographs of the entire TM circumference were captured by confocal microscopy (Carl Zeiss, Germany) to identify delivered CFSE-tagged ADSCs in the TM region. Brightfield overlays were also captured to note the corneal region and approximate TM location. Micrographs were captured as tile scans at 50x magnification and with z-stacks to account for TM depth and height differences in the tissue. Maximum intensity projections were developed for each en face image for use in further image quantification.

To determine the TM region for quantification, masks were created from brightfield images using the corneal region as a landmark. A 1mm-wide ring from the edge of the cornea mask was selected as the TM region for each image using ImageJ(22, 23). Images were further processed in Matlab (MathWorks) to remove large fluorescent debris greater than 100 µm. An example of this image analysis can be seen in Figure 2. To quantify fluorescent intensity across the TM circumference, a polar coordinate system was overlaid onto images and the total CFSE intensity was quantified for each degree. Intensities were then summed for each 10 degrees, resulting in 36 intensity values for each image. The process was repeated for non-masked fluorescent images when determining the cell signal not located in the TM.

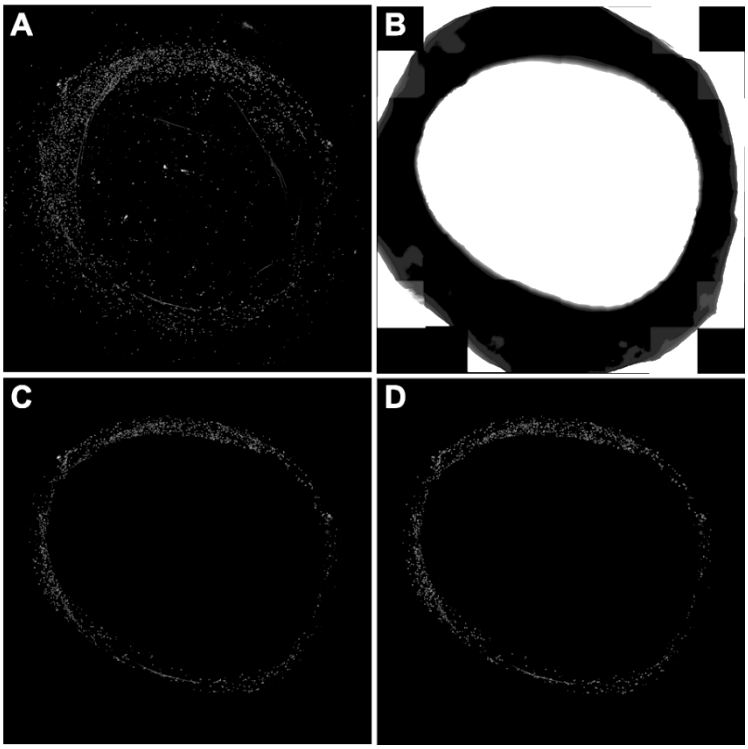

Figure 2. Image Processing Overview. (A) Raw fluorescent *en face* micrographs showing CFSE-labeled ADSCs. (B) Brightfield *en face* images used for determining the TM location. Masks were constructed from brightfield images and 1mm wide rings were used to determine (C) the TM tissue region. (D) Large fluorescent debris was excluded using Matlab before further image processing.

Cell Viability Testing

After cells were labeled with PBNCs as described above, they were stained with propidium iodide in PBS for 5 minutes at room temperature. Then, cells were detached with 0.05% trypsin/EDTA and placed in a 96-deep well plates. Cell samples were processed by flow cytometry (Attune NxT), collecting equal volumes from each sample. Living cell concentrations were determined and compared to control concentrations to determine PBNC toxicity effects.

Differentiation Tests

To determine if the PBNCs interfere with the ADSCs' ability to differentiate, ADSCs were incubated with PBNCs at ODs ranging from 0 to 2. Then, adipogenic differentiation medium or osteogenic differentiation medium was added.

After 7 days, the cells cultured in adipogenic differentiation medium were stained with Nile Red to measure lipid build-up indicating the stem cells had successfully differentiated. Cells were incubated for 5 minutes with 100 ng/mL Nile Red in PBS. Afterwards, cells were washed and probed with DAPI (Life Technologies) which fluorescently stains cell nuclei. For each cell sample, 16 fluorescent micrographs were captured in an array across each well using an imaging plate reader (BioTek, Cytation 3) and stitched together. Nile Red average fluorescent intensities were quantified for each image and normalized to DAPI cell counts. Further, adipogenesis was qualitatively assessed by Oil Red O staining(24).

After 21 days, the cells exposed to osteogenic differentiation medium were stained with Alizarin Red to stain for extracellular calcium indicating successful differentiation into an osteoblast phenotype. Cells were stained with 2% (w/v) Alizarin Red for 2 minutes followed by PBS rinses to remove excess dye. Experiments were qualitatively assessed by light microscopy followed by counterstaining cell nuclei with DAPI and 16 fluorescent images were captured using an imaging plate reader as described above.

Statistics

All in vitro studies were performed in triplicate. Analysis of variance was used to determine significance in cell experiments, where p-values less than 0.05 denote significance.

For all time points tested for cell injections, N is specified. To assess for non-uniform circular distribution towards the rectangular magnet location, Kuiper's test was performed on average results and p-values less than 0.05 indicate aggregation near the magnet location. For ring magnet experiments, Rayleigh's test for uniform circular distribution was calculated for average results and p-values less than 0.05 indicate non-uniform distribution.

CHAPTER 3

RESULTS

Proof of ADSC Labeling with PBNCs

To confirm that ADSCs were successfully labeled with PBNCs, cells were incubated with 200nm PBNCs overnight, were eosin (cytoplasm) stained, and imaged using an EVOS microscope (Figure 3). Images show blue PBNCs within the cytoplasm of the cells for all optical densities tested.

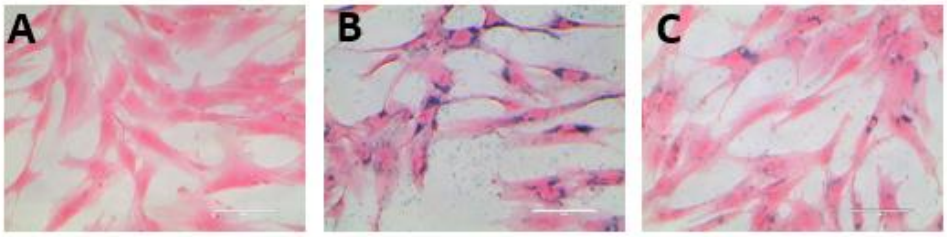

Figure 3: ADSCs labeled with PBNCs. Representative brightfield micrographs for ADSCs after incubation with different PBNC sizes and concentrations. ADSCs are eosin stained to visualize cytoplasm while PBNCs are in blue. (A) Control, (B) 2 OD, 200nm PBNC, and (C) ½ OD, 200nm PBNC.

Cell Viability Results

Flow cytometry data was gathered after propidium iodide staining two different ADSC donor strains which were labeled with PBNCs overnight (Figure 4). Data obtained was normalized to the data obtained from non-treated control cells. ADSC B showed decreased cell viability at 4 OD PBNC incubation but lower ODs showed minimal

viability effects. ADSC A did not have any significant decrease in cell viability at any of the ODs tested.

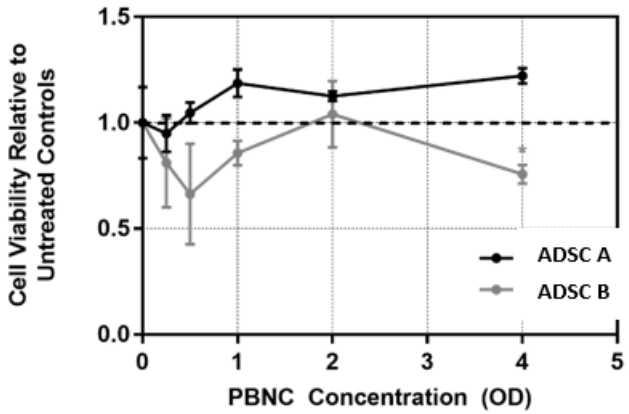

Figure 4: Live-Dead Results for 200nm PBNC labeled ADSCs. Relative viability results 1 day after PBNC labeling for 2 ADSC donor strains (n=3 for each OD). Error bars denote standard deviation.

Adipogenesis Results

Two types of ADSCs were labeled with 200 nm PBNCs and exposed to adipogenesis differentiation medium for 7 days. Oil Red O staining revealed lipid droplets inside of the cells when imaged for all optical densities as well as the control (Figure 5 A-C). The relative fluorescence when compared to untreated controls is similar, indicating little difference in differentiation between control and treatment results (Figure 5 D).

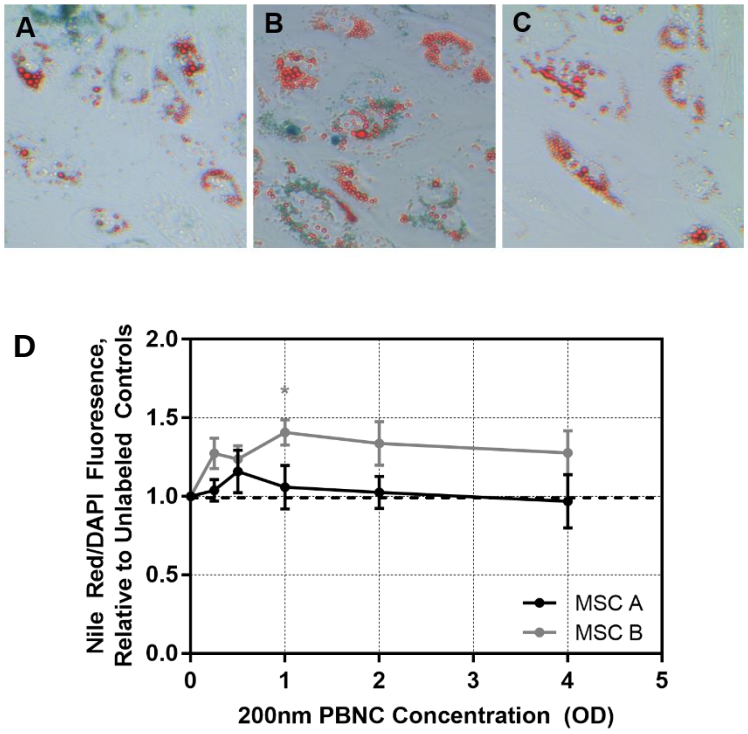

Figure 5: Effect of 200nm PBNCs on ADSC adipogenic potential. (A-C) Oil Red O (lipids) staining for (A) 4OD 200nm PBNC, (B) 1 OD 200nm PBNC, and (C) control wells 7 days after adipogenesis treatment. (D) quantification of ratio of fluorescent Nile Red (lipids) to DAPI (nuclei) signal relative to untreated controls for 2 stem cell donor strains (n=3 for each concentration). Error bars denote standard deviation.

Osteogenesis Results

Two types of ADSCs were labeled with 200 nm PBNCs and exposed to osteogenic differentiation medium for 21 days. Alizarin Red O staining revealed extracellular calcium when imaged for both optical densities as well as the control (Figure 6 A-C). The relative fluorescence data compared to the untreated controls is 1 or more for each of the cells types tested, indicating little difference in differentiation between control and treatment results (Figure 6 D).

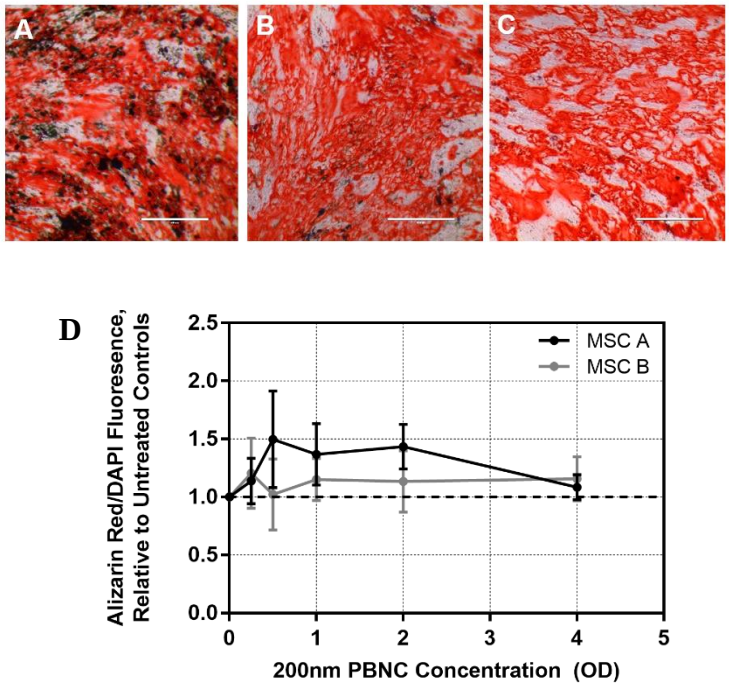

Figure 6: Effect of 200nm PBNCs on ADSC osteogenic potential. (A-C) Alizarin Red O (calcium) staining for (A) 4OD 200nm PBNC, (B) 1 OD 200nm PBNC, and (C) control wells 21 days after osteogenesis treatment. (D) quantification of ratio of fluorescent Alizarin Red (lipids) to DAPI (nuclei) signal relative to untreated controls for 2 stem cell donor strains (n=3 for each concentration). Error bars denote standard deviation.

Delivery of PBNC-labeled cells

After ADSC delivery and bar magnet exposure, *en face* micrographs were taken of the TM region. A polar coordinate system was overlaid for each resulting image (Figure 7 A). The region of the TM that was exposed to the bar magnet is centered at 0 degrees. There is much higher fluorescence seen in the magnetic quadrant following PBNC-ADSC delivery in comparison to the controls (Figure 7 A-B).

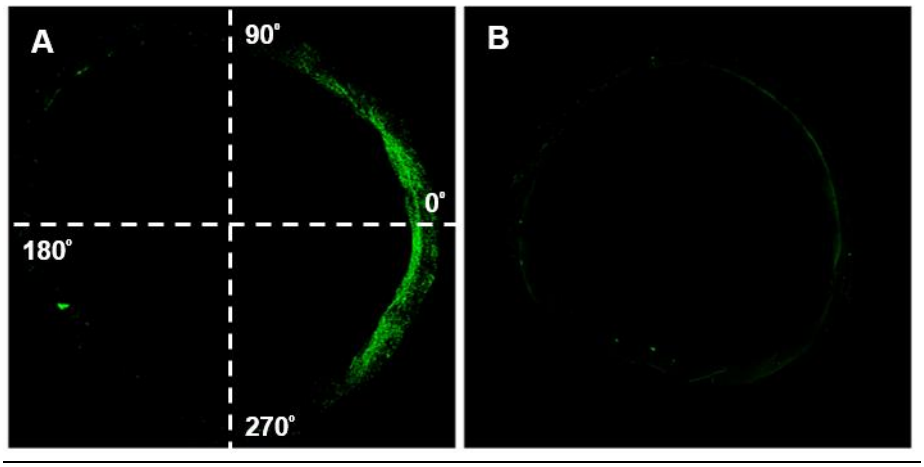

Figure 7: 200nm PBNCs for magnetic ADSC steering. Representative *en face* micrographs of the TM region following ADSC delivery and bar magnets secured overnight at 0º near the limbal region. CFSE-tagged MSCs (Green) were pre-labeled with (A) 200nm PBNCs at 2OD or (B) remained unlabeled.

Quantification of Overnight Cell Delivery

A Kuiper's test was performed on the overnight magnet exposure cell delivery images (Figure 8) to determine if there was significantly more delivery to the regions exposed to the magnet (0^o region) in comparison to the other regions. Specifically, if the region exposed to the magnet had a higher fluorescent intensity. The control ADSC injected eyes had a $p > 0.05$ and was therefore not significant. The 200nm 2 OD PBNC labeled cells each had $p < 0.001$ and were therefore significant.

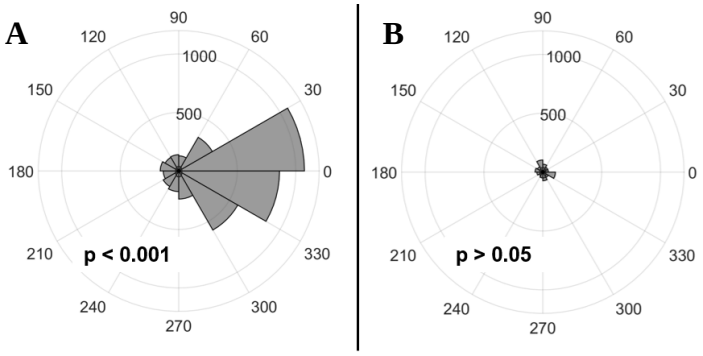

Figure 8: Quantification of ADSC delivery to the TM for 200nm PBNCs. Polar histograms illustrate ADSC fluorescent intensity (radial coordinate) for each 30º region, in which the bar magnet was place at 0º overnight. Average results (A) 200nm PBNCs at 2OD (n=4 eyes), and (B) control (n=5 eyes) experiments are shown. P-values were calculated using Kuiper's test to assess if distribution associates with 0º magnet location.

Cell delivery via ring magnet

After 2OD labeled PBNC-ADSCs were injected into eyes and then exposed to different ring magnets placed around the entire circumference for different durations, *en face* micrographs were taken of the TM region. Fluorescence shows cell delivery to the entire circumference of the TM for the eyes exposed to ring magnets (Figure 9 B-D) but not for the control (Figure 9 A).

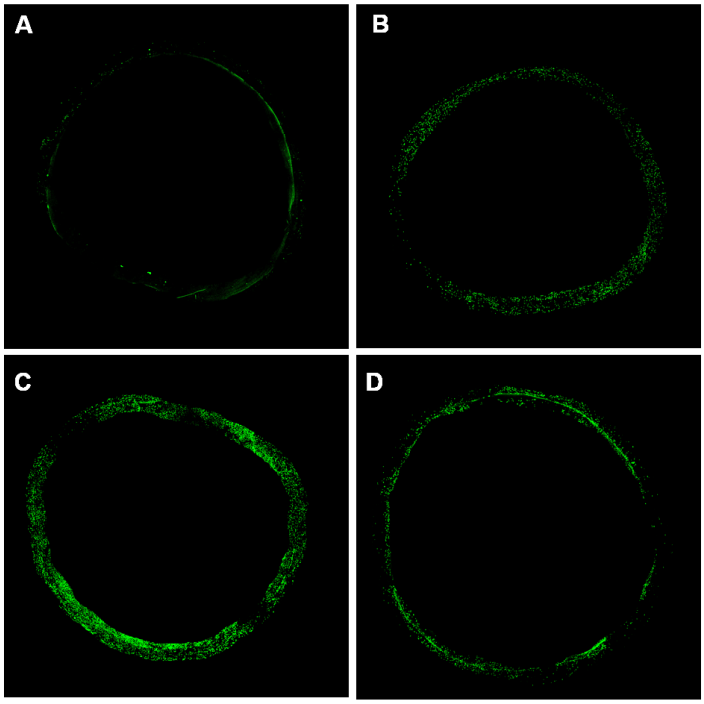

Figure 9: 360º Delivery of PBNC-ADSCs using ring magnets. 200nm, 2OD labeled PBNC-ADSCs were injected into eyes with different ring magnets placed around the entire circumference for different durations. Representative *en face* micrographs for (A) control, (B) 3D-printed magnet holder for 30 minutes, (C) axially polarized ring magnet, 15 minutes, and (D) axially polarized ring magnet, 30 minutes

Quantification of 360º cell delivery

A Rayleigh's test was performed on the ring magnet exposure cell delivery images (Figure 10) to determine if delivery was not normally distributed around the circumference, which would indicate an uneven cell delivery. The axial polarized ring magnets had $p > 0.05$ which suggesting even cell delivery (Figure 10 C-D). The Control and 3D printed custom ring magnet both had $p < 0.05$ indicating uneven cell delivery to the TM (Figure 10 A-B).

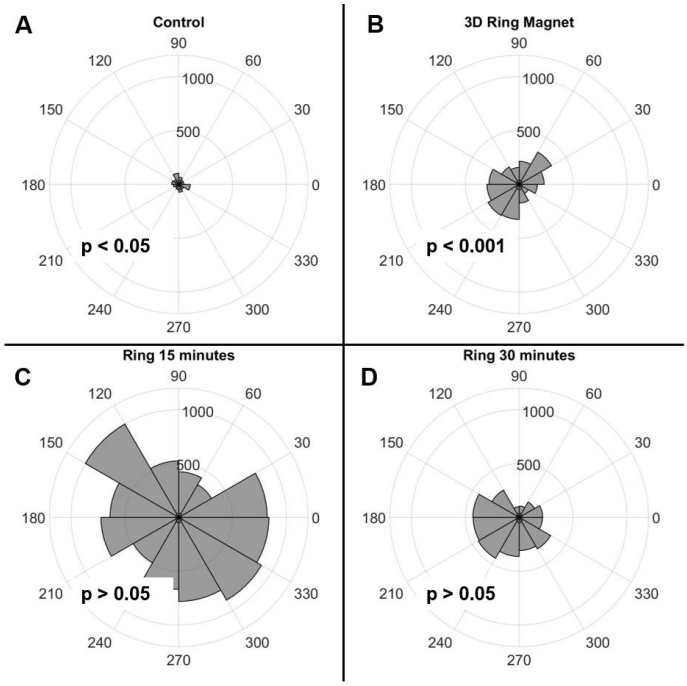

Figure 10: Quantification of ADSC delivery for ring magnet experiments. Polar histograms illustrate ADSC fluorescent intensity (radial coordinate) for each 30º region. Average results for (A) control (n=5 eyes), (B) custom-built magnet holder for 30 minutes (n=3 eyes), (C) axial polarized ring for 15 minutes (n=3 eyes), and (D) axial polarized ring for 30 minutes (n=3 eyes) experiments are shown. P-values were calculated using Rayleigh's test to assess uniform delivery ($p < 0.05$ denotes non-uniform delivery).

CHAPTER 4

DISCUSSION

The treatment of glaucoma could be greatly aided by a method to enhance stem cell engraftment to the TM for the purpose of restoring cellularity and presumably function. Restoring function to the TM would reduce resistance to AH flow and lower IOP, preventing further damage to the optic nerve. Such a method, which aims to impact the TM directly, does not currently exist. The goal of this thesis was to explore whether ADSCs which have been labeled with PBNCs can be directly targeted to the TM via magnetic field exposure.

For PBNCs to be a viable option for enhancing stem cell engraftment into the TM, they must successfully label cells. The results of the labeling experiments proved that PBNCs can enter ADSCs without prior permeabilization of the cell membrane (Figure 3). The PBNCs must also be biologically compatible with ADSCs so as not to interfere with differentiation or survival. Cell viability testing revealed that there was not significant loss in cell viability after labeling with PBNCs at the concentrations that were necessary to allow for the cells to be influenced by magnetic fields (Figure 4).

Regenerative stem cell therapies depends on stem cells differentiating into functional cells once they are delivered to the target tissue. Therefore, it is imperative that the PBNCs do not impede the ADSCs ability to differentiate. Adipogenesis and Osteogenesis assays were performed on cells that had been labeled with PBNCs (Figures 5-6). The results indicate that the ADSCs labeled with the nanoparticles were able to

successfully differentiate into both cell types to the same degree as the control cells. Overall, the tests performed for this study indicate that PBNCs can label ADSCs without affecting cell viability or differentiation. As a result, ADSCs labeled with PBNCs have the potential to be used for regenerative therapies.

Once the PBNCs had been proven to be compatible with ADSCs, we tested whether PBNC-labeled ADSCs could targeted to the TM. The cell delivery experiments indicate that PBNCs have the potential to enhance stem cell engraftment into the TM. The overnight bar magnet exposure showed that the region which was exposed to the magnet had significantly more fluorescent cell signal when compared to the rest of the TM region (Figure 8). This indicates the ADSCs labeled with PBNCs were successfully pulled to the TM region at a higher efficiency that standard delivery conditions. This proves that it is possible to use magnetic fields to direct more ADSCs to the TM compared to simply injecting ADSCs into the anterior chamber and allowing AH outflow bring cells to the TM. In addition, the ability to inject less cells decreases the number of instances in which off target binding to the cornea may occur. This decreased chance for off target delivery is important when considering the viability of this method as a potential glaucoma treatment option. If there were to be a significant amount of corneal or lens cell delivery, the ADSC therapy could worsen an individual's vision rather than helping to prevent further vision loss.

Loss of cellularity throughout the entirety of the TM occurs with both aging and glaucoma. In order for a stem cell therapy to restore function to the largest portion of the TM possible, stem cells need to be delivered to the entire circumference. Relying solely on AH outflow to deliver the cells results in delivery to only active portions of the TM during the time of delivery. These active segments are variable and are decreased in the

case of glaucoma (25). The results from the axial polarized ring magnet experiments indicate that uniform ADSC delivery to the entire circumference of the TM is possible. However, to prevent corneal binding, a better ring magnet needs to be created to more specifically aim the magnetic fields to the TM. To avoid directing cells to the cornea, a radially pulling ring magnet would be preferred. However, the 3D printed custom ring magnet used in this experiment resulted in non-uniform delivery of ADSCs to the TM circumference, so in order to optimize the magnetic field configuration of the ring magnet, further testing and refinement is needed.

CHAPTER 5

CONCLUSIONS

A therapy that directly targets the main route of AH flow in order to treat OAG does not yet exist. Stem cell therapies are a promising method to restore function and cellularity to the glaucomatous TM. In addition, using magnetic fields to allow delivery to the entire circumference of the TM will prevent cells from being delivered to the active third (or less in the case of glaucoma) of the TM and give a more adequate repair (25).

Results from these studies show PBNCs are nontoxic to ADSCs at concentrations that allow them to be pulled via magnetic fields. Further, PBNCs do not impair ADSCs ability to differentiate. Using PBNCs, ADSCs can be delivered to the TM at a higher efficiency compared to control, no magnet delivery experiments. Interestingly, PBNCs can be used to ensure an even delivery to the entire circumference of the target tissue, which may be essential for properly recellularizing the TM.

Future studies need to be done for determining why toxicity of the PBNCs in on ADSCs was different across cell strains. In addition, a better ring magnet design for pulling cells specifically to the TM needs to be developed to stop nonspecific binding of stem cells to other ocular tissues. Next steps will also involve assessing delivery *in vivo* so that other relevant anterior tissues, such as the lens and iris, can be incorporated into delivery optimization to the TM.

REFERENCES

1. Llobet A, Gasull X, Gual A. Understanding trabecular meshwork physiology: a key to the control of intraocular pressure? Physiology. 2003;18(5):205-9.
2. Abu-Hassan DW, Acott TS, Kelley MJ. The trabecular meshwork: a basic review of form and function. Journal of ocular biology. 2014;2(1).
3. Alvarado J, Murphy C, Polansky J, Juster R. Age-related changes in trabecular meshwork cellularity. Investigative ophthalmology & visual science. 1981;21(5):714-27.
4. Alvarado J, Murphy C, Juster R. Trabecular meshwork cellularity in primary open-angle glaucoma and nonglaucomatous normals. Ophthalmology. 1984;91(6):564-79.
5. Yun H, Zhou Y, Wills A, Du Y. Stem Cells in the Trabecular Meshwork for Regulating Intraocular Pressure. Journal of Ocular Pharmacology and Therapeutics. 2016;32(5):253-60.
6. Zhu W, Gramlich OW, Laboissonniere L, Jain A, Sheffield VC, Trimarchi JM, et al. Transplantation of iPSC-derived TM cells rescues glaucoma phenotypes in vivo. Proceedings of the National Academy of Sciences. 2016;113(25):E3492-E500.
7. Roubeix C, Godefroy D, Mias C, Sapienza A, Riancho L, Degardin J, et al. Intraocular pressure reduction and neuroprotection conferred by bone marrow-derived mesenchymal stem cells in an animal model of glaucoma. Stem cell research & therapy. 2015;6(1):177.
8. Manuguerra-GagnÉ R, Boulos PR, Ammar A, Leblond FA, Krosl G, Pichette V, et al. Transplantation of Mesenchymal Stem Cells Promotes Tissue Regeneration in a Glaucoma Model Through Laser-Induced Paracrine Factor Secretion and Progenitor Cell Recruitment. Stem Cells. 2013;31(6):1136-48.
9. Gao Y, Lim J, Teoh S-H, Xu C. Emerging translational research on magnetic nanoparticles for regenerative medicine. Chemical Society Reviews. 2015;44(17):6306-29.
10. Cook JR, Dumani DS, Kubelick KP, Luci J, Emelianov SY, editors. Prussian blue nanocubes: multi-functional nanoparticles for multimodal imaging and image-guided therapy (Conference Presentation)2017.
11. Rodriguez A-M, Elabd C, Amri E-Z, Ailhaud G, Dani C. The human adipose tissue is a source of multipotent stem cells. Biochimie. 2005;87(1):125-8.
12. Bunnell BA, Flaat M, Gagliardi C, Patel B, Ripoll C. Adipose-derived stem cells: isolation, expansion and differentiation. Methods. 2008;45(2):115-20.
13. Weissman IL. Stem cells. cell. 2000;100(1):157-68.
14. Zomer HD, Vidane AS, Gonçalves NN, Ambrósio CE. Mesenchymal and induced pluripotent stem cells: general insights and clinical perspectives. Stem cells and cloning: advances and applications. 2015;8:125.
15. Thomson JA, Itskovitz-Eldor J, Shapiro SS, Waknitz MA, Swiergiel JJ, Marshall VS, et al. Embryonic stem cell lines derived from human blastocysts. science. 1998;282(5391):1145-7.

16. Okita K, Ichisaka T, Yamanaka S. Generation of germline-competent induced pluripotent stem cells. nature. 2007;448(7151):313.
17. Gunsilius E, Gastl G, Petzer A. Hematopoietic stem cells. Biomedicine & pharmacotherapy. 2001;55(4):186-94.
18. Johnson TV, Bull ND, Martin KR. Identification of barriers to retinal engraftment of transplanted stem cells. Investigative ophthalmology & visual science. 2010;51(2):960-70.
19. Häfeli UO, Riffle JS, Harris-Shekhawat L, Carmichael-Baranauskas A, Mark F, Dailey JP, et al. Cell uptake and in vitro toxicity of magnetic nanoparticles suitable for drug delivery. Molecular pharmaceutics. 2009;6(5):1417-28.
20. Cores J, Caranasos TG, Cheng K. Magnetically targeted stem cell delivery for regenerative medicine. Journal of functional biomaterials. 2015;6(3):526-46.
21. Oh J, Feldman MD, Kim J, Condit C, Emelianov S, Milner TE. Detection of magnetic nanoparticles in tissue using magneto-motive ultrasound. Nanotechnology. 2006;17(16):4183.
22. Schindelin J, Rueden CT, Hiner MC, Eliceiri KW. The ImageJ ecosystem: An open platform for biomedical image analysis. Molecular reproduction and development. 2015;82(7-8):518-29.
23. Schneider CA, Rasband WS, Eliceiri KW. NIH Image to ImageJ: 25 years of image analysis. Nature methods. 2012;9(7):671-5.
24. Ramirez-Zacarias J, Castro-Munozledo F, Kuri-Harcuch W. Quantitation of adipose conversion and triglycerides by staining intracytoplasmic lipids with Oil red O. Histochemistry and Cell Biology. 1992;97(6):493-7.
25. de Kater AW, Melamed S, Epstein DL. Patterns of aqueous humor outflow in glaucomatous and nonglaucomatous human eyes: a tracer study using cationized ferritin. Archives of Ophthalmology. 1989;107(4):572-6.